Journal of Hydroscience and Hydraulic Engineering
Vol. 26, No.1 May, 2008, 29-38

FORMATION PROCESS OF DEPOSITIONAL LANDFORMS ON A PERMEABLE FLAT PLAIN

By

Motoki Ogasawara

Department of Civil and Environmental Engineering, Waseda University, Tokyo, Japan

and

Masato Sekine

Department of Civil and Environmental Engineering, Waseda University, Tokyo, Japan

SYNOPSIS

The formation process of depositional landforms on a one-dimensional permeable flat plain is investigated numerically in this paper. In this process, it is important that a water exchange between a surface flow and a subsurface flow to be taken into account. The governing equations of the flows are one-dimensional shallow water equations for surface flow and the two-dimensional Richards' equation for subsurface flow. It is found from this study that there exist the following two processes: (a) a front of surface flow migrates a little in the downstream direction due to a loss of surface flow discharge, and the thickness of depositional landforms increases; (b) the front migrates relatively rapidly due to the recovery of surface flow discharge, and the depositional landforms spread in the downstream direction. The influence of the hydraulic conductivity in the permeable layer on the formation process of depositional landforms is also investigated.

INTRODUCTION

Depositional landforms are developed when a sediment-laden flow of sand or gravel moves onto a wide plain or a permeable plain. An alluvial fan is a typical example of these landforms. When we discuss the formation mechanism, it is important to investigate the water exchange through a ground surface between a surface flow and a subsurface flow.

Studies have been conducted experimentally on the formation process of alluvial fans over four decades (for example, Hooke (2) and Schumm (4)). In these studies, depositional landforms on a laboratory scale were studied and valuable information was reported although further discussion about the scale effect is necessary. The second author of this paper also studied experimentally the formation process of depositional landforms on a permeable flat plain (Sekine et al. (5)). It was reported by Sekine et al. (5) that the pattern of sediment deposition and channel expansion on the formed landforms was chaotic due to a loss of water discharge. Referring to the literature, we found some other research on the related topics concerning water exchange between a surface flow and a subsurface

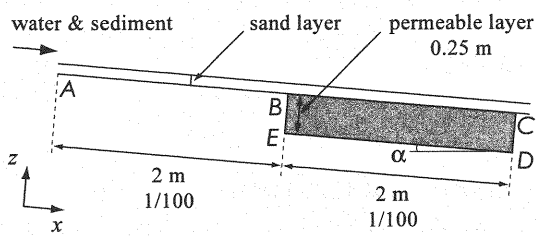

Fig. 1 Illustration of computational domain

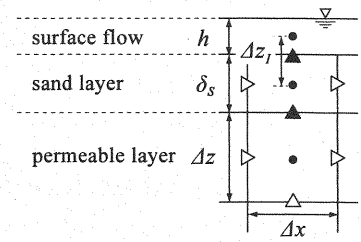

Fig. 2 Computational grid system of flow field

flow in rivers. The work by Harada (1) and Sumi, Ebara and Tsujimoto (7) are typical. However, they did not focus on the fluvial process of landforms.

The purpose of this study is to develop a numerical model which enables us to simulate the formation process of depositional landforms. To understand the mechanism of this process more precisely is another purpose of this study. A one-dimensional numerical model was constructed here as a first attempt. In this computation, the target to be analyzed is the phenomenon occurring in a flume where the bottom of the upstream half reach is impermeable and that of the downstream half reach is permeable. In the latter reach, a relatively deep "permeable layer" similar to an aquifer is located. This permeable layer is constituted of gravel. And a thin "sand layer" is also present in the entire reach, that is, on both the permeable layer and the bottom of the upstream reach. The water is supplied at the upstream end and flows downstream on the surface of this sand layer. As time passes, the front of water migrates downstream, and it reaches the downstream half reach. After that, some amount of water inflows into the permeable layer and sediment carried by the flow deposits. Finally, depositional landforms develop. Sekine et al. (5) conducted such an experiment although it was two-dimensional instead of one-dimensional. The computation here was the first attempt to simulate such a phenomenon observed by them. Furthermore, we investigated the influence of the hydraulic conductivity in the permeable layer on the formation process of depositional landforms.

NUMERICAL SIMULATION MODEL

Summary of conditions

In this study, the computational condition was set by referring to the experiment conducted by Sekine et al. (5). Fig. 1 shows an illustration of the computational domain. The area of BCDE in Fig. 1 is defined as the "permeable layer." As shown in Fig. 1, the length and the thickness of this layer were 2 m and 0.25 m, and the gradient of it was 0.01. This layer was constituted of gravel whose grain size was 5 mm in Case 1, and 2 mm in Case 2. An impermeable reach was connected to a permeable layer at the point labeled B. The length of the reach was 2 m, and the gradient of the bottom was the same as that of the permeable layer. That is, a permeable layer was located between two points at x = 2 and 4 (m). Both the bottom of the impermeable reach and the permeable layer were covered with sand whose grain size was 0.48 mm. As seen in Fig. 1, there existed a "sand layer" whose initial thickness δ_s was 0.005 m. And δ_s can vary in time and space due to deposition or erosion. Under the condition of this numerical computation, sand can be transported as bed load. The gravel which constituted a permeable layer was not exposed to a surface flow and did not move at all.

Boundary conditions are as follows. No inflow or outflow occurs through the lines of AB, BE, ED and DC in Fig. 1. At the upstream end of this computational domain, a constant discharge of water was supplied, and the discharge per unit width was 0.002 $m^3/s/m$. Sand was also supplied there by an amount estimated by substituting a dimensionless tractive force at the upstream end into a bed load function.

Table 1 Hydraulic parameters of a permeable layer and a sand layer

	grain size (m)	θ_s	θ_r	ψ_0 (m)	K_s (m/s)	m	S_s (m^{-1})
permeable layer (Case1)	5.0×10^{-3}	0.40	10^{-3}	-0.05	5.0×10^{-2}	3.0	10^{-6}
permeable layer (Case2)	2.0×10^{-3}				2.0×10^{-2}		
sand layer	0.48×10^{-3}			-0.15	0.1×10^{-2}		10^{-5}

Initial conditions are as follows. A dry bed condition was given for surface flow. The free surface of water in the permeable layer was made horizontal, and its elevation was set to be 0.05 m at x = 4(m) (see Fig. 3(a)). The initial velocity of subsurface flow was zero.

In Table 1, the hydraulic parameters of porous media in a permeable layer and a sand layer are shown. The exponent m in Eq. 5 was 3.0, which was estimated theoretically by Irmay (3). Moreover, the value of Manning's coefficient was 0.03, and the value of dimensionless critical tractive force for sand was 0.032.

Surface flow

In this study, the depth of surface flow is so small (less than 13 mm) that the so-called "shallow water assumption" is effective. Therefore, the governing equations of surface flow are one-dimensional shallow water equations:

$$\frac{\partial h}{\partial t}+\frac{\partial hu}{\partial x}=w_I \tag{1}$$

$$\frac{\partial u}{\partial t}+u\frac{\partial u}{\partial x}+\frac{uw_I}{h}=g\sin\alpha-g\cos\alpha\left(\frac{\partial h}{\partial x}+\frac{\partial \eta}{\partial x}\right)-\frac{C_f}{h}u^2+\frac{\partial}{\partial x}\left(\nu_t\frac{\partial u}{\partial x}\right) \tag{2}$$

where h is a flow depth, u is a depth-averaged velocity, g is gravitational acceleration, α is the angle between the x-axis and a horizontal line, η is a bed elevation and ν_t is a turbulent diffusion coefficient, respectively. w_I is a flux (volumetric flow rate per unit area) through the interface between a surface flow and a subsurface flow. If the inflow from a surface flow to a subsurface flow occurs, w_I takes a negative value. If the outflow from a subsurface flow to a surface flow occurs, on the other hand, w_I takes a positive value. C_f is a friction coefficient and in this study was evaluated by Manning's law.

Subsurface flow

A flow of water in unsaturated porous media is governed by both a continuity equation and the equations of flow velocity which is a modified Darcy's law. Substituting the equations of flow velocity into the continuity equation, the so-called Richards' equation is derived. We can evaluate the flow field in both an unsaturated and a saturated porous media by this equation. In this study, the phenomenon in a vertical x-z plain was analyzed and the following two-dimensional version of Richards' equation was solved numerically:

$$\left(\frac{\partial\theta}{\partial\psi}+\beta S_s\right)\frac{\partial\psi}{\partial t}=\frac{\partial}{\partial x}\left\{K\left(\frac{\partial\psi}{\partial x}-\sin\alpha\right)\right\}+\frac{\partial}{\partial z}\left\{K\left(\frac{\partial\psi}{\partial z}+\cos\alpha\right)\right\} \tag{3}$$

where θ is volumetric water content, ψ is a pressure head, S_s is a specific storage coefficient and K is hydraulic conductivity, respectively. The x and z coordinates are taken as is seen in Fig. 1. And the coefficient β in this equation is defined as follows: β=1 if the value of ψ is positive or zero, and β=0 if the value of ψ is negative.

In order to solve Eq. 3, we need to determine the relationships among the parameters ψ, θ and K. The relationship between ψ and θ derived by Tani (8) was adopted:

$$\theta = (\theta_s - \theta_r)\left(\frac{\psi}{\psi_0} + 1\right) exp\left(-\frac{\psi}{\psi_0}\right) + \theta_r \tag{4}$$

and the relationship between θ and K used by Tani (8) was adopted in this study:

$$K = K_s \left(\frac{\theta - \theta_r}{\theta_s - \theta_r}\right)^m \tag{5}$$

where θ_s is saturated water content, θ_r is residual water content, ψ_0 is a pressure head giving the maximum value of $\partial\theta/\partial\psi$, K_s is saturated hydraulic conductivity and m is an exponent in Eq. 5.

Modeling of a water exchange

In this computation, the following vertical structure is assumed: (a) a permeable layer constituted of gravel, (b) a sand layer on it, and (c) the space for surface flow above the sand layer. Therefore, the subsurface flow in the two layers of (a) and (b) was calculated. Water exchange through the interfaces between (a) and (b) and between (b) and (c) were evaluated in a following manner.

The flux through the upper surface of the sand layer, which corresponds to the interface between (b) and (c), is defined as w_1 in Eqs. 1 and 2. This flux is evaluated on the basis of the so-called Darcy's law and is calculated by

$$w_1 = \begin{cases} -K_s\left(\dfrac{\psi_u - \psi_d}{\Delta z_1} + cos\alpha\right); & if \quad h > 0 \\ 0; & if \quad h = 0 \end{cases} \tag{6}$$

In Eq. 6, K_S is saturated hydraulic conductivity of the sand layer, ψ_u is the pressure head evaluated by hydrostatic pressure distribution in the flow depth of surface flow, ψ_d is the pressure head in the sand layer, and Δz_1 is the distance in the z direction between these two points (see Fig. 2).

The flux through the interface between a sand layer and a permeable layer, which corresponds to the interface between (a) and (b), was evaluated in the same manner as aforementioned. The hydraulic conductivity at the interface is evaluated as a smaller value of the two, that is, the value of either the sand layer or the permeable layer.

Sediment transport

Bed load is only considered here as a type of sediment transport. The bed load transport rate was evaluated by Meyer-Peter and Müller's formula. The "slope collapse model" by Sekine (6) was introduced to evaluate an additional sediment transport rate. The local angle of depositional landforms grows larger as it develops, and then the angle reaches tentatively an angle of repose of sediment in this computation. In fact, such a steep slope collapses before the above condition is satisfied. We can calculate such an event reasonably by this slope collapse model, and a local angle is maintained not to exceed the angle of repose. The sediment volume yielded by this collapse is treated as an additional sediment transport. The bed elevation at each grid point is calculated by solving Exner's equation, and the additional sediment transport rate as well as that evaluated by Meyer-Peter and Müller's formula is considered. For further details, the reader may refer to the original paper by Sekine (6).

Summary of computation

The procedures of this computation are as follows: (1) a subsurface flow is analyzed first; (2) a surface flow is analyzed by considering the value of w_1 which is estimated by using a latest value of pressure head of subsurface

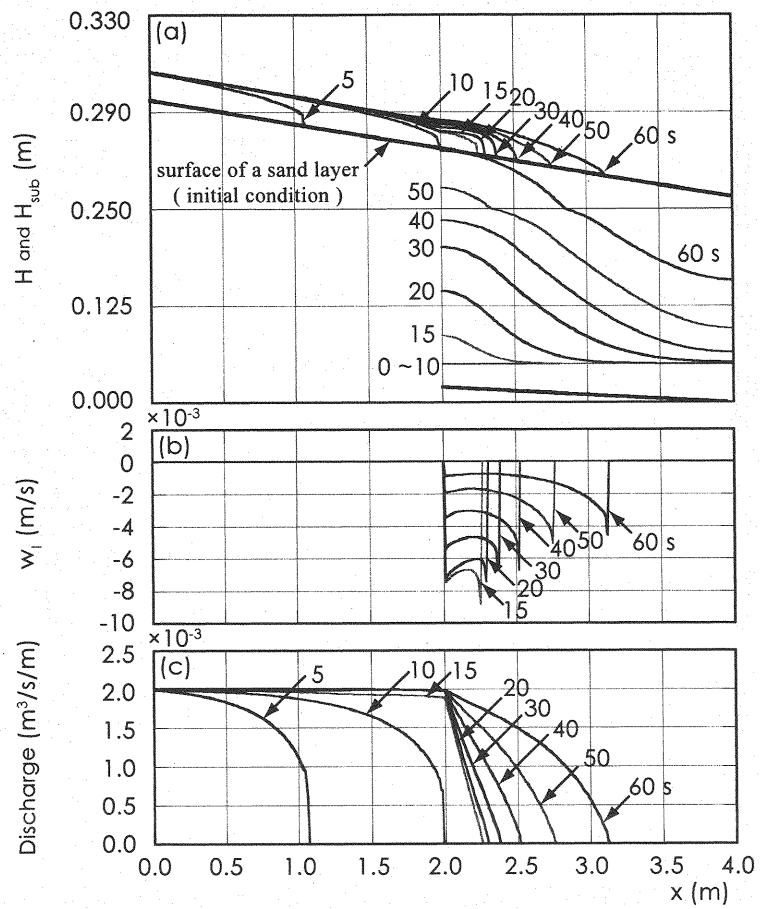

Fig. 3 Summary of the numerical results (Case 1) : (a) water surface elevation of surface flow H and free surface elevation of subsurface flow H_{sub}, (b) the flux through the interface between surface flow and subsurface flow w_1, (c) the discharge of surface flow. The number in each figure denotes the time from the beginning of computation. The permeable layer is located between x=2 and 4 (m).

flow; (3) after such computations of the flow, the deformation of bed elevation is evaluated. These are the computations every single time step. The time interval Δt was set to be 0.0005 s in this analysis. Moreover, the distances between each node of the computational grids in the x and z direction Δx and Δz were set to be 0.01 m.

In solving governing Eqs. 1 and 2 for surface flow, the following individual solution techniques were adopted: (a) the staggered grid system, (b) the explicit scheme, and (c) the CIP scheme for a convective term. In solving Eqs. 3-5 for subsurface flow, on the other hand, the fully implicit scheme and the successive over relaxation (SOR) method were adopted.

RESULTS

Formation process of depositional landforms

The formation process of depositional landforms is discussed in this section with referring to the numerical results of Case 1.

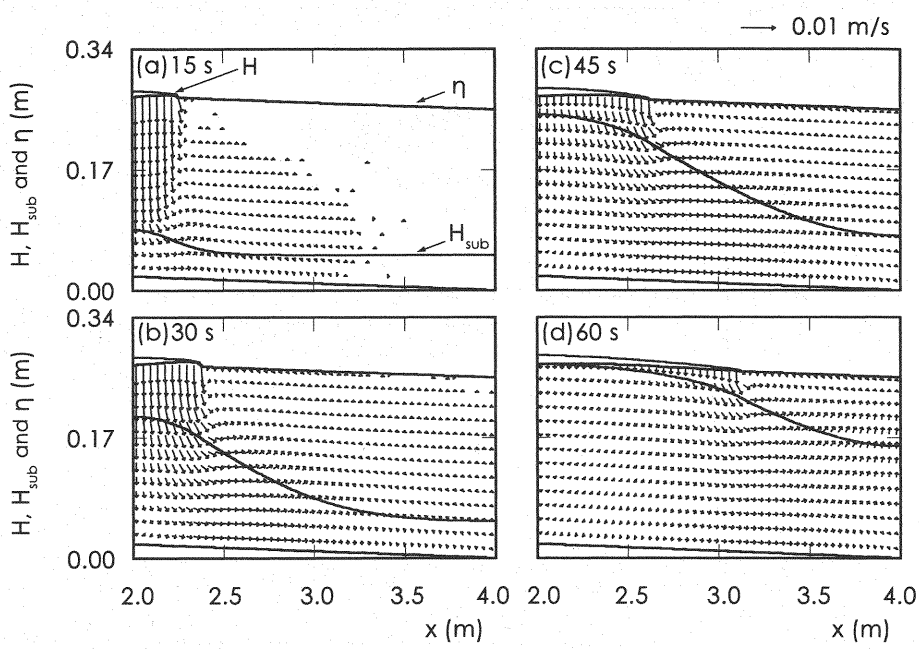

Fig. 4 Velocity vectors of subsurface flow (Case 1) : (a) 15 s, (b) 30 s, (c) 45 s and (d) 60 s from the beginning of computation.

Fig. 3(a) shows a time series of water surface profiles. The upper lines correspond to the profiles of surface flow, and the lower lines correspond to the free surface profiles of subsurface flow. We can see from this figure that a water front of surface flow migrates downstream, but the movement is not continuous. The pattern of surface flow migration can be described briefly as follows: (1) A front of surface flow migrates downstream with almost constant speed until the front reaches the point x = 2 (m) at which there exists an upstream boundary of the permeable layer. The reason for the migration is that a water discharge keeps constant and no net loss of water discharge occurs due to the impermeability of the upstream half reach. (2) The front reaches the point x = 2 (m) at about 10 s, and then it migrates with its speed slowed down till about 15 s. (3) The front migrates by a small distance approximately from 15 s till 30 s. It looks as if it stops during this period. (4) After that, the front starts to migrate again relatively rapidly.

Fig. 3(b) denotes temporal and spatial variations of the flux w_l through the interface between a surface flow and a subsurface flow. Fig. 3(c) shows the variations of surface flow discharge. In Fig. 4, the velocity vector maps of subsurface flow are seen. It is obvious from both Fig. 3(b) and Fig. 4 that the influx from a surface flow to a subsurface flow is dominant and causes an increase of moisture in the permeable layer. This results in the rise of the free surface in this layer. Fig. 3(c) shows, on the other hand, that discharge of surface flow decreases in the downstream direction on the permeable bed due to this influx. Moreover, we can see from Fig. 3(c) that the surface flow discharge on the permeable bed increases as the magnitude of the flux w_l in Fig. 3(b) decreases. As we expected, it is recognized from both Fig. 3(b) and Fig. 3(c) that the flux w_l and the discharge of surface flow are closely related.

In Fig. 5, the profiles of the amount of bed deformation $\Delta\eta$ are seen. In this study, a bed is equivalent to the surface of landforms. Fig. 5 shows that depositional landforms develop on the permeable bed after the front of surface flow reaches the upstream end of the bed (x=2(m)). The discharge of surface flow decreases on the permeable bed, as was explained above. Therefore, the reach appeared where a tractive force decreases in the

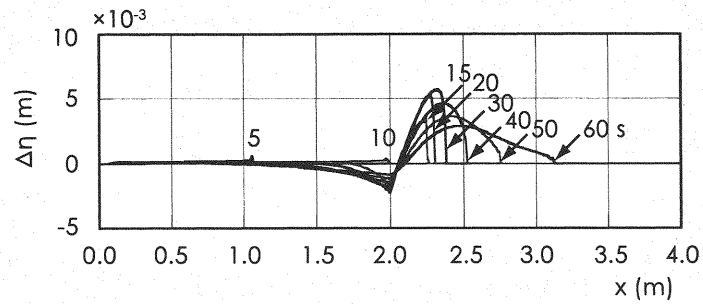

Fig. 5 Profiles of the amount of bed deformation Δη from initial bed (Case 1). Each number in this figure denotes the time from the beginning of computation.

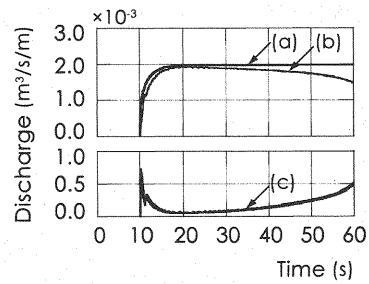

Fig. 6 Temporal variation of discharges (Case 1) : (a) the discharge of surface flow at x = 2.0 (m), (b) the inflow discharge from a surface flow to a subsurface flow and (c) the difference between the above two discharges.

downstream direction on the permeable bed due to the decrease of surface flow discharge. Sediment deposition occurs in this reach. Erosion occurs, on the other hand, in the reach where a tractive force increases. The pattern of landform development can be described briefly as follows: (1) The deposited area extends further in the downstream direction and the landforms migrate downstream. (2) In the upstream reach the landforms are eroded and they become thinner. Such a phenomenon became evident after approximately 30 s, when the water front of surface flow started to migrate again.

From the findings explained above, we found that there are two stages in the development of depositional landforms, especially in the one-dimensional case. One is the initial stage, and the water front of surface flow almost stays still and does not migrate considerably in the downstream direction due to the discharge loss of surface flow. At this stage, depositional landforms develop in a restricted area, but they grow thicker as time passes. In this computation, this stage corresponds to the period between 15 s and 30 s approximately. Fig. 6 shows the temporal variations of discharge. Line (a) in this figure denotes a surface flow discharge at the upstream end of the permeable bed (x=2(m)), and line (b) is the inflow discharge from a surface flow to a subsurface flow. The difference between the above two discharges is denoted as line (c) in this figure. If the difference between two discharges is equal to zero, the front of surface flow stops completely except when a slope collapse occurs. In this computation, the front of surface flow did not stop completely and migrated by a small distance because the surface flow discharge at the point of x=2(m) was always larger than that of the inflow by a small amount. At the second stage, the water front continues migrating downstream. As is seen in Fig. 6, the discharge of surface flow is much larger than inflow discharge into a permeable layer at this stage, and the depositional landforms continue to expand. In the case of the present computation, this stage began at about 30 s. Therefore, the migrating speed of surface flow tends to increase.

Under the conditions of this study, the above two sub-processes including a transition from one to the other were

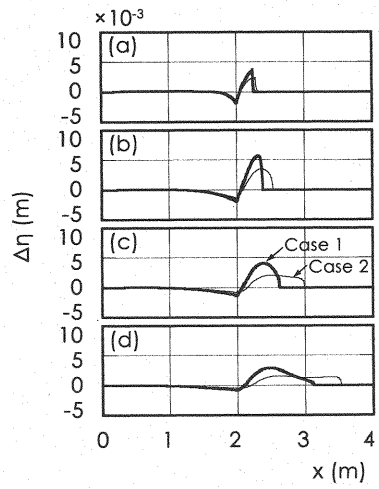

Fig. 7 Profiles of the amount of bed deformation Δη : (a) 15 s, (b) 30 s, (c) 45 s and (d) 60 s from the beginning of computation.

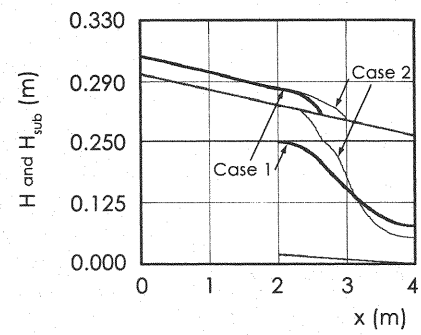

Fig. 8 Water surface profiles of surface flow and the free surface profiles of subsurface flow at 45 s.

observed. According to the results of the computations under different conditions, we found that only one of the two sub-processes appeared. For example, if the vertical walls at both upstream and downstream ends of the permeable layer (lines BE and CD in Fig. 1) are replaced by a permeable one, a free surface of subsurface flow can rise so little that the process in the initial stage only appears. If the initial elevation of free surface of subsurface flow is close to the upper end of permeable layer, on the other hand, the discharge loss of surface flow is so little that the process in the second stage only appears, and depositional landforms do not develop significantly. In addition to the above two sub-processes, some other processes were observed. For example, a "return flow" occurred from a certain point toward the downstream direction. The so-called "wadi" or "dried-up river" also appeared in the upstream reach of the point.

Influence of the hydraulic conductivity in the permeable layer on the formation process of depositional landforms

In this section, the influence of the hydraulic conductivity in the permeable layer on the formation process of depositional landforms is discussed. Numerical conditions are explained in Table 1. Hydraulic conductivity in the permeable layer of Case 1 is larger than that of Case 2. In Figs. 7 and 8, the numerical results of both Case 1 and Case 2 are shown. The thick lines in these figures denote the results of Case 1, and the thin lines, on the other hand, denote the ones of Case 2. Fig. 7 shows the profiles of the amount of bed deformation Δη at each time. It can be seen from this figure that the thickness of depositional landforms of Case 1 is larger than that of Case 2. And the migrating distance of the landforms of Case 1 is smaller than that of Case 2. The reason why such differences occur in the formation process of depositional landforms is discussed here. If the hydraulic conductivity is smaller and a downward flux in the upper part of the permeable layer is smaller than the inflow from the surface flow, a moisture rise in the upper part occurs more quickly. Therefore, the free surface of subsurface flow in Case 2 rose earlier than that in Case 1. Fig. 8 shows both the water surface profiles of surface flow and the free surface profiles of subsurface flow at 45 s from the beginning of the computation. We can see from Fig. 8 that a sand layer as well as a permeable layer were completely saturated in the upstream reach of x = 2.2 (m) in Case 2, but there was no such saturation zone in Case 1. This indicates that the reduction in the water discharge of surface flow grows moderate earlier,

and the recovery of the discharge arises more dominantly in Case 2. Therefore, the front of surface flow migrates further in Case 2 than in Case 1. As a result, it can be concluded that the depositional landforms can extend further downstream and their thickness grows smaller as the hydraulic conductivity takes a smaller value.

CONCLUSION

The formation process of depositional landforms on a permeable flat plain was investigated in this study. A numerical simulation model was developed to simulate the process on a one-dimensional plain as a first attempt. In conclusion, it was verified qualitatively that the numerical model worked well and that the mechanism of the process was understood to some extent. From the numerical simulation, the following conclusions are obtained:

(1) We found the following two sub-processes in the formation of landforms. At the initial stage, a front of surface flow migrates a little in the downstream direction due to the discharge loss of surface flow, and the thickness of depositional landforms increases. After that, the front migrates relatively rapidly due to the recovery of surface flow discharge, and the depositional landforms spread in the downstream direction. This is the second stage.

(2) The landforms grow larger in scale in the downstream direction and thinner as the hydraulic conductivity of porous media in permeable layer is smaller.

The numerical model will be extended to a two-dimensional one in order to simulate an alluvial fan formation, just as in the experiment conducted by Sekine et al. (5). Verification of the numerical model quantitatively will be also conducted by comparing the results with that of experiment. These matters will be the subject of our next investigation though there still remain some problems for us to overcome.

REFERENCES

1. Harada, M. : Hydraulic analysis on stream-aquifer interaction by storage function models, Journal of Hydraulic, Coastal and Environmental Engineering, JSCE, No.628/II-48, pp.189-194, 1999 (in Japanese).
2. Hooke, R.L. : Process on arid-region alluvial fans, Journal of Geology, Vol.75, pp.438-460, 1967.
3. Irmay, S. : On the hydraulic conductivity of unsaturated soils, Trans. AGU, Vol.35, pp.463-467, 1954.
4. Schumm, S.A. : The Fluvial System, John Wiley & Sons, pp.255-264, 1977.
5. Sekine, M., Arai, T. and Kubota, Y. : Fluvial depositional landforms on permeable plain, Annual Journal of Hydraulic Engineering, JSCE, Vol.42, pp.1087-1092, 1998 (in Japanese).
6. Sekine, M. : Numerical simulation of braided stream formation on the basis of slope-collapse model, Journal of Hydroscience and Hydraulic Engineering, JSCE, Vol.22, No.2, pp.1-10, 2004.
7. Sumi, T., Ebara, U. and Tsujimoto, T. : On the sub-surface flow and water exchange rate through temporary ponds on a sandbar, Advances in River Engineering, JSCE, Vol.6, pp.89-94, 2000 (in Japanese).
8. Tani, M. : The properties of a water-table rise produced by a one-dimensional, vertical, unsaturated flow, Journal of Japanese Forestry Society, Vol.64, pp.409-418, 1982 (in Japanese).

APPENDIX-NOTATION

The following symbols are used in this paper:

C_f = friction coefficient;

g = gravitational acceleration;

h = flow depth;

K = hydraulic conductivity;

K_s = saturated hydraulic conductivity;

m = exponent in Eq. 5;

S_s = specific storage coefficient;

t = time;

u = depth averaged velocity;

w_I = flux through the interface between a surface flow and a subsurface flow;

α = the angle between the x-axis and a horizontal line;

β = coefficient in Eq. 3;

δ_s = thickness of sand layer;

Δt = time interval;

Δx = grid size in the x direction;

Δz = grid size of the permeable layer in the z direction;

Δz_I = distance in Eq. 6;

η = bed elevation;

θ = volumetric water content;

θ_r = residual water content;

θ_s = saturated water content;

ν_t = turbulent diffusion coefficient;

ψ = pressure head;

ψ_0 = pressure head which gives the maximum value of $\partial\theta/\partial\psi$;

ψ_d = pressure head in the sand layer in Eq. 6; and

ψ_u = pressure head evaluated by flow depth of surface flow in Eq. 6.

(Received Jun 29, 2007 ; revised Sep 21, 2007)